

# Properties of serendipitous X-ray flares discovered in *XMM – Newton* observations

Duncan Trenholme, Gavin Ramsay, Carl Foley

*Mullard Space Science Laboratory, University College London, Holmbury St. Mary, Dorking, Surrey, RH5 6NT, UK*

Received:

## ABSTRACT

We present the results of a search of the *XMM-Newton* public data archive for stellar X-ray flares. We find eight flaring sources for which we identify 7 optical counterparts. Three of these sources have distance estimates which allow us to determine their luminosities. Based on the decay time of the flares and their luminosity we derive loop half-lengths of  $\sim 2 - 7 \times 10^{10}$  cm and emission measures of  $\sim 10^{54}$  cm $^{-3}$ : these are similar to values derived for other stellar flaring sources. One of the stars shows two flares in close succession. We discuss the likelihood of this double event being either sympathetic or homologous in nature. A comparison to a pair of similar flares on the Sun suggests that homology is the more likely process driving the flare event.

**Key words:** Sun: flares, corona – stars: activity, coronae, flare – Galaxy: open clusters and associations: – X-rays: stars, binaries

## 1 INTRODUCTION

Solar and stellar flares have been studied using both ground and space observatories. Solar observations have revealed that the energy source which powers Solar flares most probably originates with the destruction and reconnection of Solar magnetic fields, as they relax to a lower energy configuration (Priest & Forbes 1999). The excess of energy which was stored in the stressed pre-flare Solar magnetic field is released in an outburst over most of the electromagnetic spectrum, from Radio through to X-ray.

Flares which have been observed on stellar sources, are substantially more powerful than their Solar counterparts by many orders of magnitude (eg Stern, Underwood & Antiochos 1983). These include T-Tauri stars where the young rapidly rotating protostar has a relatively high magnetic field. The magnitude and frequency of the flares typically reduce as the protostar enters the main sequence. This has been attributed to the reduction in their rotation rate, which results in a slowing of the stars internal dynamo, the process responsible for generation of stellar magnetic fields.

Flare stars are usually discovered as a result of intensity variability studies. One systematic search was that of the *ROSAT* all sky survey which revealed 767 X-ray variable stars many of which were found to be flare stars with both long duration flare activity and sporadic short flare activity (Fuhrmeister & Schmitt 2003). Whilst this survey was unbiased, it was impossible to study the temporal vari-

ation of the flares in any detail since the duration of each observation was short.

In contrast, the longer orbit of *XMM-Newton* allows uninterrupted observation of sources for many hours. Further, *XMM-Newton* has the largest effective area of any imaging X-ray satellite, and in comparison with *ROSAT*, has a much broader energy band and a higher spectral resolution. A search of the *XMM-Newton* data archive provides an excellent opportunity to conduct a search for new sources which are flaring in X-rays. Each flare can be studied in detail and will add to the increasing database on X-ray stellar activity in general.

In this paper we present the results of our search for stellar flares using the serendipitous *XMM-Newton* data held in the public archive. We show the results of our analysis of these flares which include an estimate of their luminosity and the nature of the source from which it originated. We estimate the loop half-length of four flares, and compare our results with that of other stellar flares. We also investigate the process which may have caused a double flare event which was observed on one of the sources and then compare its properties with Solar flare events.

## 2 OBSERVATIONS

*XMM-Newton* was launched in Dec 1999 by the European Space Agency (Jansen et al. 2001). The EPIC instruments have imaging detectors covering the energy range  $\sim 0.15$ -

arXiv:astro-ph/0409217v1 9 Sep 2004

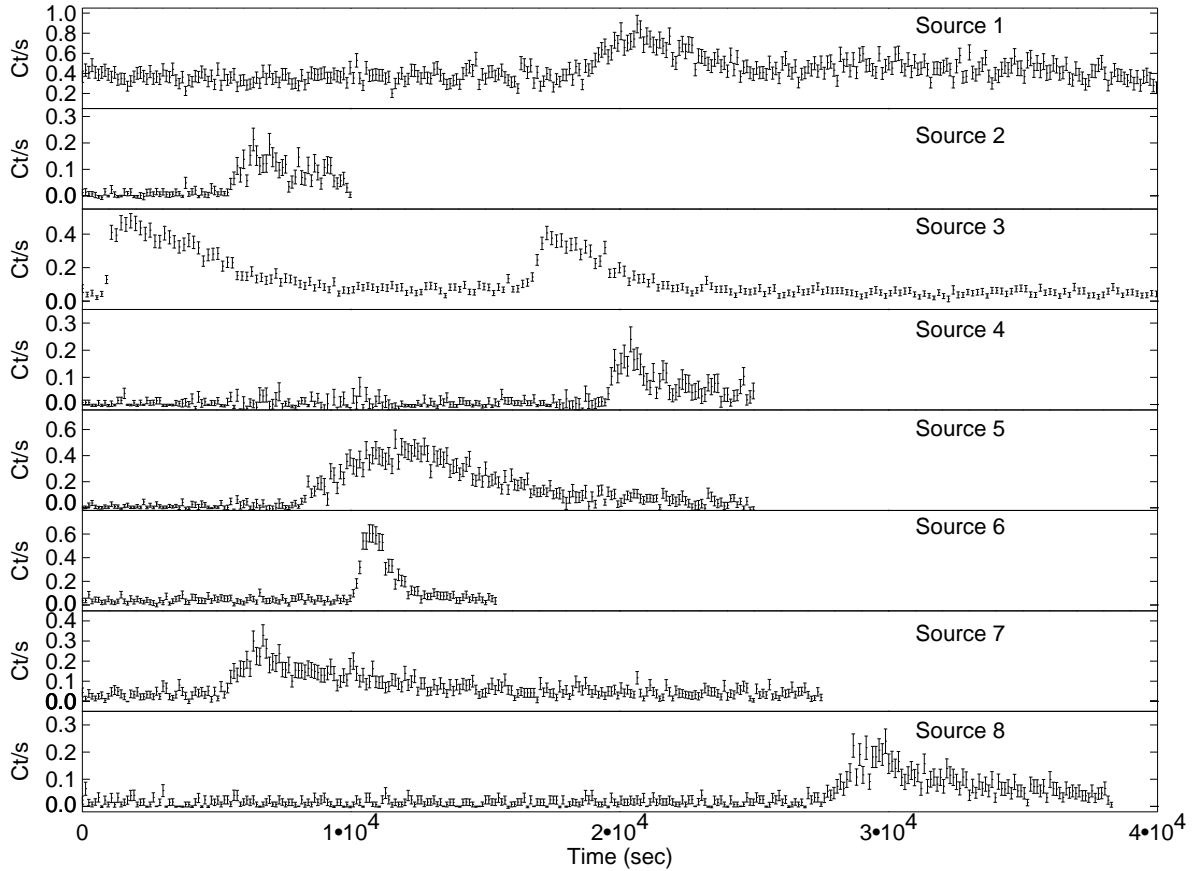


**Figure 1.** The background subtracted X-ray light curves for each of the 8 flares in the energy range 0.2–5.0 keV. All light curves are extracted from the EPIC pn instrument, apart from Source 3, which is from the EPIC MOS 1+2 instrument. The bin size is 120 sec for all except Source 3 which is 180 sec

Date	Orbit	ObsId	Clean Time (ksec)
2002-02-20	0403	0007422401	9.0
2002-03-24	0419	0112640201	21.7
2002-06-15	0461	0041750101	51.6
2002-08-13	0490	0101440201	50.4
2002-09-15	0507	0112530101	34.0
2002-09-15	0507	0049560301	13.8
2002-12-16	0553	0148440101	25.0

**Table 1.** The observation log for the selected *XMM-Newton* observations. We show the date of the observation, the *XMM-Newton* orbit number, the observation id and its clean time duration.

10 keV with moderate spectral resolution. Since our main interest is searching for X-ray flares: we therefore use data primarily taken using the EPIC pn detector since this has the highest effective area of the imaging X-ray detectors (Strüder et al. 2001). All the observations for this search were selected from the *XMM-Newton* public data archive. The selected observations were chosen with bias toward fields that potentially contained a large number of X-ray sources, and bias against fields that contained clusters of galaxies, since they were less likely to contain flaring sources (for brevity we do not note the individual fields which were

selected). In this paper we present the results of our analysis of the first 100 observations we selected from the *XMM-Newton* public data archive.

The data were processed using the *XMM-Newton* Science Analysis Software (SAS) v5.3.3. Each field was source searched and the light curve of each detected source was tested for variability (see Ramsay, Harra & Kay 2003 for details of this procedure). A total of 8 sources were found to show clear flare-like variability, ie a rapid (less than a few ksec) increase in the X-ray count rate followed by a decline lasting less than  $\sim 10$  ksec. For these sources we obtained background-subtracted light curves, typically with a bin-size of 120 sec. Table 1 shows the *XMM-Newton* observation logs for the fields which contained these flares. Other sources were found to be variable, but did not show flare-like behaviour.

Using the SIMBAD Astronomical database and the USNO-B1.0 optical catalogue, we searched for optical counterparts of our X-ray flaring sources. For seven of our eight sources we found a counterpart (Table 2). The offset between the *XMM-Newton* and optical counterpart was typically less than 3 arcsec. This is significantly less than the FWHM of sources in the EPIC pn. We note in Table 2 the USNO catalogue number of each source, the *B* and *R* magnitudes from two epochs, and the *V* and *B* magnitudes from SIMBAD. There is evidence that some of these sources show significant variation in their optical brightness between epochs. We have not identified a optical counterpart to Source 8,

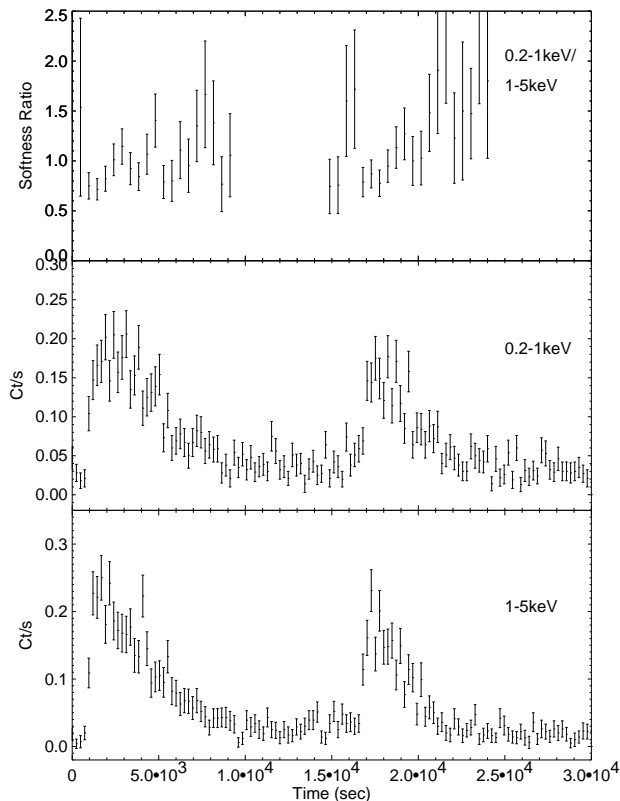


**Figure 2.** The double flare seen on Source 3 in the 0.2–1 keV (middle panel) and 1–5 keV (bottom panel) and the 0.2–1/1–5 keV softness ratio (top panel).

although it is located in the immediate vicinity of  $\zeta$  Ori, which may have prevented optical surveys reaching as deep as usual.

### 3 LIGHT CURVES

In Figure 1, we present the background-subtracted X-ray light curves for each flaring source we found. The light curves resemble those of typical Solar flares, some being impulsive (Sources 2, 3, 4 and 6), long duration (Source 5) and intermediate (Sources 1, 7 and 8) in nature.

The sources with impulsive flares all show a rise to their maximum brightness on a timescale of  $\sim 500$  sec. The flare on Source 6 is particularly short, lasting less than  $\sim 1$  hr (the time duration for which flux is observed to be above the normal quiescent level), while for Source 2 and 4 the observation finishes before the end of the flare. In comparison Sources 7 and 8 show a rise time approximately 4 times as long as the rapid flares, with the decay time also being relatively long, indeed the decay continues beyond the end of the observation.

In contrast, in Source 5, the rise to maximum is much more gradual than the sources already discussed, and the maximum lasts much longer. Source 1 differs to the other sources in that a significant flux is seen before the increase in flux, with the light curve profile being broadly similar in shape to Source 5.

Perhaps the most interesting of the sources is the third, which displays two impulsive flares of similar size and du-

ration, separated by  $\sim 4$  hours 20 mins. (The EPIC MOS 1+2 light curve has a longer time duration than the EPIC pn light curve, so the MOS 1+2 light curve is shown in Figure 1). The first flare lasts for  $\sim 150$  mins while the second flare lasts for a slightly shorter time, with a duration of  $\sim 120$  mins. (This flaring source is briefly alluded to by Pillitteri et al. 2004 in an analysis of the same *XMM-Newton* dataset).

To investigate this double flare in more detail we extracted a background-subtracted light curve in the 0.2–1 and 1–5 keV energy bands. We show these light curves and the resulting softness curve in Figure 2. The softness ratio curve shows evidence for a softening over the duration of both flares. This is consistent with the flare observed from JTP 138 in NGC 2516 (Ramsay et al. 2003).

### 4 SOURCE SPECTRA

We extracted spectra for each of the 9 flares found on the 8 sources, using the time interval of the flare duration only. For each flare a background spectrum was also extracted from a nearby source-free area of the detector. Since the sources were not on-axis we generated response and auxiliary files for each source using the SAS tasks `rmfgen` and `arfgen`. Further, we used only good events (`FLAG=0`) and single and double events (`PATTERN=0–4`). The spectrum was then fitted using the X-ray package `XSPEC` (Dorman & Arnaud 2001).

We initially fit all spectra using an absorbed thermal plasma model. All spectra required the addition of a second thermal plasma component to achieve good fits. We show the results of the spectral fits for all the flares in Table 3. We note that these results may be affected as a result of spectral softening over the duration of the stellar flares (c.f. Figure 2). We also show the observed flux in the 0.1–10 keV band and for those sources for which we know the distance (§5) we show the bolometric luminosity for the flare. We find the low temperature plasma has a temperature  $kT \sim 0.7$  keV, and a range of temperature for the hotter plasma component. In some sources, the fits were significantly improved when we allowed the metal abundance of the plasma to vary from Solar (Table 3). There is no relationship between metal abundance and observed flux, suggesting that this effect is not simply related to the signal-to-noise ratio of the spectrum.

We show the spectrum of the brightest flare (Source 5) in Fig. 3: the fit is good with no evidence of significant residuals at particular energies. This source was also the only system to show evidence for an Fe line at  $6.6^{+0.3}_{-0.2}$  keV: this may simply be due to the fact that the other spectra have lower signal-to-noise ratios, especially at higher energies. We note that the brightest flaring source in NGC 2516 (JTP 138) also showed an Fe line consistent with this line energy (Ramsay et al. 2003).

We show the average flare luminosity for 4 flares in Table 3. These range between  $6\text{--}34 \times 10^{30}$  ergs s $^{-1}$ . The most luminous flare is Source 6, although since it is of short duration the total energy released is comparable to the less luminous flares. However, at its brightest it is an order of magnitude more luminous than the flare source JTP 138 in NGC 2516.

Source	RA (2000.0)	Dec	USNO-B1.0	$V$	$(B - V)$	Magnitude $B_1$ $B_2$ $R_1$ $R_2$	XMM Obs ID
1	10 42 41.5	-64 21 05	0256-0180983	10.62	0.64	10.50 11.09 11.45 11.47	0101440201
2	13 57 03.4	-58 47 10	0312-0398114			16.92 14.92 15.28	0007422401
3	00 02 56.4	-30 04 46	0599-0000714	12.13	0.85	13.54 13.00 11.31 12.15	0041750101
4	05 42 12.3	-02 05 10	0879-0104649	15.7		16.58 15.58 14.95 14.64	0112640201
5	05 41 45.5	-02 24 17	0875-0105863			21.13 19.14 19.40	0112640201
6	05 35 22.3	-04 25 28	0855-0060617	6.25	-0.15	5.96 6.14 6.30 6.32	0049560301
7	01 40 31.3	-68 05 09	0219-0011450			14.69 12.74 12.71	0148440101
8	05 40 52.5	-02 00 48					0112530101

**Table 2.** The X-ray sources which showed significant X-ray variability in our survey. The X-ray position is the position from the XMM-Newton EPIC pn image. The  $V$  and  $(B - V)$  mag are taken from SIMBAD, while  $B$  and  $R$  magnitudes are from the USNO-B1.0 catalogue at 2 epochs. We also indicate the XMM-Newton observation number (cf Table 1) in which the source was detected.

Source	$N_H$ $\times 10^{20} \text{ cm}^{-2}$	$kT_1$ (keV)	$kT_2$ (keV)	Abundance $Z_\odot$	Observed flux $\text{ergs s}^{-1} \text{ cm}^{-2}$	Bolometric luminosity $10^{30} \text{ ergs s}^{-1}$ $10^{34} \text{ ergs}$	$\chi^2_\nu$ (dof)
1	$10^{+2}_{-2}$	$0.7^{+0.0}_{-0.1}$	$7.8^{+9.9}_{-3.2}$	0.07	$1.52^{+0.42}_{-0.36} \times 10^{-12}$	$9.3^{+2.6}_{-2.2}$ $7.5^{+2.0}_{-1.8}$	1.18 (116)
2	$0.2^{+1.8}_{-0.2}$	$0.7^{+0.4}_{-0.3}$	$2.8^{+1.2}_{-0.6}$	1	$5.38^{+1.22}_{-0.94} \times 10^{-13}$		0.57 (11)
3a	$0.7^{+1.0}_{-0.7}$	$0.7^{+0.0}_{-0.1}$	$2.1^{+0.3}_{-0.2}$	0.34	$8.35^{+1.82}_{-1.57} \times 10^{-13}$	$8.8^{+1.9}_{-1.6}$ $9.7^{+2.1}_{-1.8}$	1.09 (95)
3b	$1.8^{+1.4}_{-1.6}$	$0.7^{+0.1}_{-0.1}$	$1.7^{+0.5}_{-0.3}$	0.15	$5.14^{+2.92}_{-2.57} \times 10^{-13}$	$6.2^{+4.2}_{-3.0}$ $5.6^{+3.8}_{-2.7}$	0.82 (55)
4	$8.3^{+4.9}_{-3.8}$	$0.9^{+0.1}_{-0.2}$	$\geq 4.5$	0.08	$6.90^{+3.83}_{-4.15} \times 10^{-13}$		1.21 (18)
5	$5.2^{+1.1}_{-1.0}$	$0.7^{+0.1}_{-0.4}$	$5.0^{+0.7}_{-1.0}$	1	$2.32^{+0.07}_{-0.18} \times 10^{-12}$		1.23 (101)
6	$3.3^{+2.5}_{-1.9}$	$0.6^{+0.1}_{-0.2}$	$5.2^{+1.7}_{-1.2}$	1	$1.83^{+0.22}_{-0.21} \times 10^{-12}$	$34.3^{+4.3}_{-4.0}$ $17.5^{+2.1}_{-2.1}$	1.23 (29)
7	$0.7^{+1.3}_{-0.7}$	$0.9^{+0.1}_{-0.1}$	$\geq 1.95$	0.08	$6.04^{+3.35}_{-3.17} \times 10^{-13}$		1.54 (39)
8	$3.9^{+4.0}_{-2.4}$	$0.4^{+0.2}_{-0.1}$	$3.3^{+0.1}_{-0.1}$	1	$4.26^{+0.72}_{-0.70} \times 10^{-13}$		1.14 (28)

**Table 3.** The spectral fits to the 9 X-ray flares. We have extracted events covering only flare time interval.

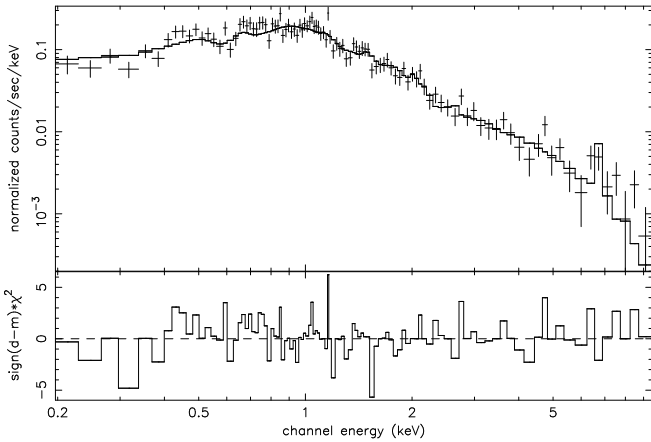


**Figure 3.** The EPIC pn spectrum of Source 5. The best fit (shown as a solid line) is an absorbed two temperature plasma model.

## 5 THE NATURE OF THE SOURCES

We have identified seven of the eight sources as having an optical counterpart. Of these, 3 are situated in the same field as known open clusters.

Source 3 is in the same field as the open cluster Blanco 1. To determine the likelihood of Source 3 being a member of this cluster we compared the  $V$ ,  $B - V$  data of the source with the locus of the main sequence (de Epstein & Epstein 1985) of Blanco 1: we conclude that this source is very likely a cluster member. For the calculation of the luminosity of

the flares from Source 3, a distance of 262 pc was used (the distance to Blanco 1, Robichon et al. 1999). Panagi et al. (1994) found ambiguous optical spectroscopic evidence for binarity in this source.

Four other sources in this cluster were flagged as being X-ray variable with a confidence of  $>99\%$  (Micela et al. 1999). Lightcurves were extracted for the three sources that were found within the XMM-Newton field of view. Two of these sources were found to significantly vary within the observation, both between 0.1 and 0.5 ct/sec, but they did not show flare-like behaviour.

Source 6 is identified with the bright star HD37016. It has a distance of 346 pc based on the HIPPARCOS catalogue (Perryman et al. 1997). It has a B2.5V spectral type and is a member of the cluster NGC 1977.

Source 1 is the only other of the eight sources to be classified spectroscopically. Braes (1962) found this source to have a G0 spectral type. Barnes et al. (1999) identify this source as a variable star with period  $0.57 \pm 0.01$  days: it was also noted that the optical lightcurves suggest the differential rotation of migrating starspots. The source is located in the field of cluster IC 2602. Based on comparisons with  $V$ ,  $R - V$  data of the main sequence (Prosser, Randich & Stauffer 1996) we conclude this source is very likely to be a member of this cluster. The source was also found to have a radial velocity consistent with membership (Randich et al. 1997). The distance to cluster IC 2602 is 150 pc (Prosser et al. 1996) which we used in the calculation of the luminosity of the flare event for this source.

Source 4 is an emission line star, with  $V \sim 15.7$ , which

was found to be near nebulosity (Wiramihardja et al. 1989). There is another optical source identified within one arcsecond of this source and is highly reddened and much fainter ( $V \sim 20$ ) compared to the counterpart identified in Table 2. The two sources cannot be resolved on the Digital Sky Survey image. Source 7 was found to be an X-ray source in the Wide Angle ROSAT Pointed Survey (Perlman et al. 2002).

Various systems exhibit flare like behaviour similar to the sort we have observed in the sources presented here. These include late main sequence stars; Young Stellar Objects (YSOs); RS CVn binary systems; single early type stars; and binaries containing M dwarf stars. Single late type main sequence stars usually show flare luminosities orders of magnitude less than those reported here (e.g. Tsikoudi, Kellelt, & Schmitt 2000). Although YSOs show flare luminosities and intensity profiles consistent with those three sources for which we have distance estimates, Sources 1 and 3 are located in open clusters in which star formation has ceased and are therefore unlikely to be YSOs. In contrast Source 6 is located in the Orion star forming region, indicating that it may be a YSO. RS CVn systems, binary systems containing an M dwarf, or single early type stars, have flare luminosities similar to that observed for our sources. To settle the nature of these objects, a short series of medium resolution spectra is necessary.

## 6 FLARE ANALYSIS

Soft X-ray observations have revealed that the Sun consists of many hot X-ray emitting coronal loops which trace the coronal magnetic field. Flares occur when these loop systems interact by a process of magnetic reconnection (Priest & Forbes 1999). This often occurs as a result of the emergence of magnetic flux into pre-existing coronal loops, or due to a shearing of loop foot-points, with both phenomena producing flares with different characteristics and sizes. We are not currently able to spatially resolve stellar coronae, and therefore it is difficult to determine the nature of stellar flares directly. However, it is possible to get an estimate of the sizes of the emitting volume and stellar coronal loops from the timescale of the flare decay (Serio et al. 1991).

If we assume that the flare plasma cools predominantly by radiation and that heating takes place at the impulsive phase of the flare with no additional heating, we can equate the observed flare e-folding decay time with the radiative cooling time  $t_{rad}$ . Serio et al. 1991 discuss the applicability of this first assumption, while the latter is generally the case for impulsive flares. For a flare with a temperature  $T$  the average electron density of the flare  $n_e$  is given by

$$n_e = \frac{3kT}{t_{rad}P(T)} \quad (1)$$

where  $k$  is the Boltzmann constant and  $P(T)$  is the radiative loss function for a unit emission measure. Mewe, Gronenschild & van den Oord (1985) showed that for flares with temperature higher than 20MK this function can be approximated as  $P(T) \sim 10^{-24.73} T^{0.25} \text{erg cm}^3 \text{s}^{-1}$ . We can use the flare temperatures which we derived from our spectral fits (see Table 3) to make estimates of the electron density (shown in Table 4).

Based on our spectral fits we have also determined the

Source	$EM$ ( $10^{53} \text{cm}^{-3}$ )	$t_{rad}$ (ks)	$n_e$ ( $10^{11} \text{cm}^{-3}$ )	$L$ ( $10^{10} \text{cm}$ )
1	8.7	4.6	4.5	2.6
3a	5.8	4.0	1.9	4.0
3b	5.3	3.4	2.0	3.7
6	13.8	1.2	1.3	6.9

**Table 4.** Estimates for the loop half length ( $L$ ) of the four flares which a distance to the source was established. Also shown is the e-folding decay time ( $T_{rad}$ ), an estimate for the electron density ( $n_e$ ), and a calculation of the emission measure ( $EM$ ).

emission measure ( $EM$ ) for the four flares from sources with known distances. Pallavicini, Tagliaferri & Stella (1990) have shown that this can be expressed for a flare composed of  $n_L$  loops each with an average length  $L$ , as

$$EM = n_L n_e^2 (2\pi\beta^2 L^3) \quad (2)$$

where  $\beta$  is the ratio between radius of the loop cross-section and its semi-length. Typical values of  $\beta$  for Solar coronal loops are  $\sim 0.1 - 0.3$  (Golub et al. 1980). We have used the above relationship, assuming the emission originates from a single coronal loop, to derive the loop half-lengths for the four flares which we have presented in Table 4.

To understand the significance of these estimates, and draw any conclusions about the nature of the flares on these stars it is necessary to know the stellar radii,  $R_s$ . We use the spectral type of Source 1 and 6 as found in §5, and the mass of Source 3 as  $\sim 1.10 M_\odot$  (Pillitteri et al. 2003) to estimate the stars radius assuming they are on the main sequence (Allen 1973). We find that Source 1 and Source 3 both have  $R_s \sim 1.05 R_\odot$ , while Source 6 is much larger  $R_s \sim 5.3 R_\odot$ . The length of the flare loop estimated for Source 1 is therefore  $\sim 0.7 R_s$ , for Source 6 it is  $\sim 0.4 R_s$ , while for both flares on Source 3 the loop is of the order of the stellar radii.

Solar flares originating from coronal loops of the order of a Solar radii are relatively uncommon, and are generally associated with transequatorial loop flares between different active regions (Glover et al. 2003). These flares are generally found to be very faint, and are very difficult to distinguish from the average full Solar X-ray flux. The brightest Solar flares are often very compact ( $L \sim 0.05 R_\odot$ ), usually being composed of multiple compact loops and often forming arcades (Pallavicini et al. 1990). It is possible that the large flares observed on Source 3, are in fact due to magnetic reconnection in a combination of multiple smaller loops, rather than one excessively large loop. If we assume average loop half-lengths of  $\sim 0.05 R_s$ , this would suggest  $n_L \sim 20$ .

## 7 INVESTIGATION INTO THE DOUBLE FLARE

Source 3 showed two rapid impulsive flares during the same observation, in contrast with all the other sources which showed only one. Flares on the Sun are observed frequently, at many wavelengths and over many timescales, as a result of continuous observation. Prominent Solar flares are sometimes observed within a short time interval: they can be described in a sympathetic or homologous way.

Sympathetic flares are thought to occur when a flare ini-

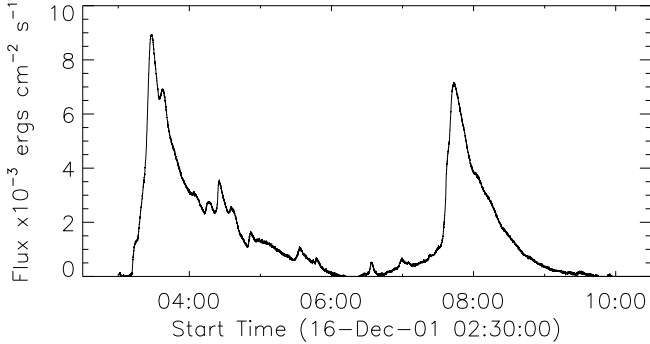


**Figure 4.** A double Solar flare event in the wavelength range 1–8Å (1.5–12.4 keV). The flare took place on Dec 16 2001.

tiates a shock front, a coronal disturbance, which propagates to another active region on the Solar disk causing that active region to flare. These disturbances are known as Moreton waves (Moreton 1964), and are observed in the chromosphere typically traveling at Alfvénic speeds. The shocks are normally followed by a slower moving density enhancement in the corona, which travels at about a third of the Alfvén speed (Chen et al. 2002). Another way in which active regions may communicate is via conduction fronts which propagate along magnetic structures linking remote regions (Švestka et al. 1977).

Homologous flares are caused by the recurrent destruction and reformation of the stellar magnetic fields, driven by the constant action of emerging flux and/or magnetic shear (Martres et al. 1984). This often produces flares of similar magnitude and emission measure which originate from the same active region. We now investigate whether either of these processes are occurring in Source 3.

### 7.1 Sympathetic Activity

Using the procedure detailed in §4 we extracted a spectrum for the quiescent state of Source 3 (assumed to be after the end of the second flare). We found the spectrum could be fitted with a single temperature plasma model with  $T_{\text{quiescent}} = 0.8 \text{ keV}$ . Brown, Melrose & Spicer (1979) showed that the speed of a conduction front can be given by the ion sound speed

$$c_i = \sqrt{\frac{kT}{m_i}} \quad (3)$$

where  $m_i$  is the mean mass of an ion (Brown et al. 1979). Here, we take  $T$  to be  $T = T_{\text{flare}} - T_{\text{quiescent}}$ . For a difference in temperature of  $\sim 1.5 \times 10^7 \text{ K}$ , (as determined for Source 3), a conduction front would propagate at a speed of  $\sim 320 \text{ km s}^{-1}$ .

Pearce & Harrison (1990) studied flare activity of 15 different active regions on the Sun, and found that active region pairs separated by less than  $\sim 35^\circ$  displayed significant amounts of coincident flaring, while much less correlation was found between more widely separated pairs.

Recalling our estimate of the stellar radii of Source 3, from the previous section ( $R_s \sim 1.05 R_\odot$ ), a conduction front travelling at a speed of  $\sim 320 \text{ km s}^{-1}$ , from the first flare on Source 3 would have reached active regions with more than a  $\sim 35^\circ$  separation in just  $\sim 25$  mins. It would take even less

Solar Flare	EM ( $10^{52} \text{ cm}^{-3}$ )	T (KeV)	Luminosity ( $10^{26} \text{ ergs s}^{-1}$ )	( $10^{30} \text{ ergs}$ )
1	2.1	0.7	1.3	1.3
2	1.7	0.6	1.3	1.1

**Table 5.** The Emission Measure, average Temperature, and luminosity for the two Solar flares observed by GOES on December 16 2001.

time if the propagation from the first flare was instead a Moreton wave, which typically travel in the range  $500\text{--}1000 \text{ km s}^{-1}$  on the Sun (Moreton 1964). We find that at a speed of  $\sim 320 \text{ km s}^{-1}$  the conduction front from the first flare on source 3 would have travelled across the whole stellar disc in just over  $\sim 2$  hours, which is a little under half of the delay time of 4 hours and 20 mins observed between the two flares. Even if there were significant errors in the estimates of stellar radius and the conduction front speed, it is highly unlikely that the second flare is sympathetic to the first.

### 7.2 Homology, a comparison with Solar flares

We searched a section of the *X-ray sensor* (XRS) archives from the *Geostationary Operational Environmental Satellites* (GOES) satellite for Solar flare activity that had a similar temporal profile and interval between flares as seen on Source 3. In Figure 4, we present the lightcurve of two such Solar flares that were observed by GOES on 2001 December 16. We used the ratio of the counts recorded in the 1.5–12.4 keV and 3–25 keV energy bands of GOES (Figure 4), to measure the average emission measure, and electron temperature of the two Solar flares, (see Table 5). The derived luminosity was found to be the same in both Solar flares:  $\sim 1.3 \times 10^{26} \text{ ergs s}^{-1}$ .

The two Solar flares both show a rapid rise to peak brightness with longer decay times. The decay time is shorter in the second of the two flares,  $\sim 130$  mins as opposed to  $\sim 160$  mins in the first flare. The second flare is also at a lower temperature and has a smaller emission measure than the first flare (see table 5) There is a delay time of  $\sim 4$  hours 20 mins between the peak brightness of each flare. The characteristics mentioned above are all consistent with those found on the double flare event observed on Source 3.

We examined the images of the flares from the *Soft X-ray imager* (also on GOES) and the *Extreme ultraviolet Imaging Telescope* (on the *Solar and Heliospheric Observatory*). Both flares have a similar morphology and appear to originate from the same active region, NOAA 9733, (with a GOES classification of M1.0 and C8.5 respectively). This, coupled with the similar luminosity of each flare, indicates that the flares are homologous in nature.

This suggests that the stellar double flares which we observed on Source 3, may be homologous in nature and from the same stellar active region. The only significant difference between the stellar and Solar case is that the stellar flares seen on Source 3 have emission measures and temperatures larger than the flares seen on the Sun. This could be explained by the existence of a stronger magnetic field in the stellar active region. According to the chromospheric evaporation model of Shibata & Yokoyama (1999), a factor

of  $\sim 100$  difference in the respective magnetic field strengths could explain the larger luminosity of the stellar flares.

## 8 CONCLUSIONS

We have searched the *XMM-Newton* public data archive for sources showing X-ray flares. We found 8 objects which show light curves with flare like behaviour showing that the *XMM-Newton* archive is an excellent resource with which to find such objects. We extracted the EPIC PN spectra (0.2–10 keV) for each of the events and derived physical parameters such as temperature, emission measure and flux. Using the optical identification we estimated distances to three of the sources, permitting calculations of the flare luminosity and an estimate of the flare loop half-lengths. These are consistent with previous estimates of flaring coronal loops on other stellar sources.

Source 3 showed two flares of similar magnitude and duration. We estimate that the loop length of each flare is approximately the length of the stellar radius. It is also possible the flare is composed of many smaller flare loops, as is often observed on the Sun. In this case, we estimate the number of loops to be of the order of 20.

We have investigated the origin of this ‘double’ flare by making an analogy with a Solar double flare event which had a light curve similar to the one on Source 3. We have explored whether the process driving these flares were sympathetic or homologous in nature. An estimate of the speed of a conduction front propagating over the stellar surface, along with our estimate of the stellar radius excludes the possibility that these stellar flares are sympathetic in nature. On the other hand an investigation of the similar Solar event implies it is likely that we are observing homologous flares from just a single stellar active region on Source 3. In this scenario, the interval observed between the flares reflects the time required for the reconfiguration of the corona back to the original pre-flare state, thus permitting the region to flare again under the same conditions and resulting in a similar flare event. The major difference between the comparable Solar and stellar observation is the magnitude of the flare event, which can be attributed to a stronger stellar magnetic field of the order of a  $100\times$  the Solar magnetic field.

## 9 ACKNOWLEDGMENTS

The authors would like to thank Louise Harra, Sarah Matthews, Lydia van Driel-Gesztelyi, Hilary Kay and David Williams for helpful discussions and suggestions. DT would like to thank Mark Cropper for helpful comments and also for supporting his work placement at the Mullard Space Science Laboratory, enabling the work presented in this paper to be done. This paper is based on observations obtained with *XMM-Newton*, an ESA science mission with instruments and contributions directly funded by ESA Member States and the USA (NASA), and made use of archival material from SIMBAD, which is operated at CDS, Strasbourg. This research has also made use of the USNO-B1.0 catalogue using the HEASARC search page. We thank the referee for helpful comments.

## REFERENCES

- Allen, C. W., 1973, *Astrophysical Quantities*, Athlone Press  
 Barnes S.A., Sofia S., Prosser C.F., Stauffer J.R., 1999, *ApJ*, 516, 263  
 Braes L.L.E., 1962, *Bull. Astron. Inst. Neth.* 16, 297  
 Brown J.C., Melrose D.B., & Spicer D.S., 1979, *ApJ*, 228, 592  
 Chen P.F., Wu S.T., Shibata, K., Fang C., 2002, *ApJL*, 572, L99  
 Dorman B., Arnaud K.A., 2001, in Harden F.R., Primi F.A., Payne H. E., eds, *ASP Conf. Ser. Vol. 238, Astronomical Data Analysis Software Systems X*. Astron. Soc. Pac., San Francisco, p.415  
 de Epstein A.E.A., Epstein I., 1985, *AJ*, 90, 1211  
 Fuhrmeister B., Schmitt J. H. M. M., 2003, *A&A*, 403, 247  
 Glover A., Harra L.K., Matthews S.A., & Foley C.A., 2003, *A&A*, 400, 759  
 Golub L., Maxson C., Rosner R., Vaiana G.S., Serio S., 1980, *ApJ*, 238, 343  
 Jansen F., et al., 2001, *A&A*, 365, L1  
 Martres M.-J., Mein N., Mouradian Z., Rayrole J., Schmieder B., Simon G., Soru-Escout I., Woodgate B.E., 1984, *AdSpR*, 4, 5  
 Mewe R., Gronenschild E.H.B.M., van den Oord G.H.J., 1985, *A&AS*, 62, 197  
 Micela G., Sciortino S., Favata F., Pallavicini R., Pye J., 1999, *A&A*, 344, 83  
 Moreton G., 1964, *Symposium the physics of solar flares*, ed Hess W.N., NASA-SP20  
 Pallavicini R., Tagliaferri G., Stella L., 1990, *A&A*, 228, 403  
 Panagi P.M., O’Dell M.A., Collier Cameron A., Robinson R.D., 1994, *A&A*, 292, 439  
 Pearce G., Harrison R.A., 1990, *A&A*, 228, 513  
 Perlman E.S., Horner D.J., Jones L.R., Scharf C.A., Ebeling H., Wegner G., Malkan M., 2002, *ApJS*, 140, 265  
 Perryman M.A.C. et al., 1997, *A&A*, 323, L49  
 Pillitteri I., Micela G., Sciortino S., Favata F., 2003, *A&A*, 399, 919  
 Pillitteri I., Micela G., Sciortino S., Damiani F., Harnden Jr. F. R., 2004, accepted *A&A*, astro-ph/0403303  
 Priest E., Forbes T., 1999, *Magnetic Reconnection*. Cambridge Univ. Press, Cambridge  
 Prosser C.F., Randich S., Stauffer J.R., 1996, *AJ*, 112, 649  
 Ramsay G., Harra L.K., Kay H., 2003, *MNRAS*, 341, 1388  
 Randich S., Aharpour N., Pallavicini R., Prosser C.F., Stauffer J.R., 1997, *A&A*, 323, 86  
 Robichon N., Arenou F., Mermilliod J.-C., Turon C., 1999, *A&A*, 345, 471  
 Serio S., Reale F., Jakimiec J., Sylwester B., Sylwester J., 1991, *A&A*, 241, 197  
 Shibata K., Yokoyama T., 1999, *ApJ*, 526, L49  
 Stern R.A., Underwood J.H., Antiochos S.K., 1983, *ApJ*, 264, L55  
 Strüder L. et al., 2001, *A&A*, 365, L18  
 Švestka Z., Krieger A.S., Chase R.C., Howard R., 1977, *SoPh*, 52, 69  
 Tsikoudi V., Kellett B.J., Schmitt J.H.M.M., 2000, *MNRAS*, 319, 1136  
 Wiramihardja S.D., Kogure T., Yoshida S., Ogura K., Nakano M., 1989, *PASJ*, 41, 155